Abstract

An accurate and direct algorithm for solving the semiclassical Boltzmann equation with relaxation time approximation in phase space is presented for parallel treatment of rarefied gas flows of particles of three statistics. The discrete ordinate method is first applied to discretize the velocity space of the distribution function to render a set of scalar conservation laws with source term. The high order weighted essentially non-oscillatory scheme is then implemented to to capture the time evolution of the discretized velocity distribution function in physical space and time. The method is developed for two space dimensions and implemented on gas particles that obey the Maxwell-Boltzmann, Bose-Einstein and Fermi-Dirac statistics. Computational examples in one- and two-dimensional initial value problems of rarefied gas flows are presented and the results indicating good resolution of the main flow features can be achieved. Flows of wide range of relaxation times and Knudsen numbers covering different flow regimes are computed to validate the robustness of the method. The recovery of quantum statistics to the classical limit is also tested for small fugacity values.

Semiclassical Boltzmann-BGK Equation, Discontinuous Galerkin Methods, Discrete Ordinate Method

A Discontinuous Galerkin Method for Initial Value Problems of Rarefied Gas Flows of Arbitrary Statistics

Jaw-Yen Yang[1] and Min-Hung Chen[2]

November 2, 2012

1 Introduction

In kinetic theory of gases, the Boltzmann equation has been widely used to describe various transport phenomena in classical rarefied gas covering wide range of flow parameters such as Reynolds number, Mach number and Knudsen number. The Chapman-Enskog expansion method is usually applied to the Boltzmann equation to derive closed set hydrodynamic transport equations that apply to a broad range of flow regimes, see [**?**]. In analogy to the classical Boltzmann equation, a semiclassical Boltzmann equation, which generalizes the collision term in order to treat the collision of particles of quantum statistics, has been developed; For detail, readers may refer to [**?**,**?**]. Hydrodynamic behaviour of quantum gases has been the subject of some prominent researches, see [**?**,**?**,**?**], and the application of quantum Boltzmann hydrodynamic equations have been implemented in the analysis of electron flows in quantum semiconductor devices, such as in the works of [**?**, **?**, **?**]. In recent years, due to the rapid advancements of microtechnology and nanotechnology, the device or structure characteristic length scales become comparable to the mean free path and the wavelength of energy and information carriers (mainly electrons, photons, phonons, and molecules), some of the classical continuum transport laws are no longer applicable. It is generally believed that the microscopic description of Boltzmann equation (classical and semiclassical) is adequate to treat transport phenomena in the mesoscale range. Different types of carriers may involve simultaneously in a single problem, therefore, it is desirable to have a method that can allow one to treat them in a unified and parallel manner. Indeed, this is the view advocated in micro- and nano-scale energy transport by Chen [**?**]. With the semiclassical Boltzmann equation, it is possible to describe adequately the mesoscale transport of particles of arbitrary statistics.

The principal difficulty encountered in solving semiclassical Boltzmann equation as derived by Uehling and Uhlenbeck is the same as that encountered in the classical counterpart and is mainly due to the complicated integral nature of its collision term. The relaxation time approximation proposed by Bhatnagar, Gross and Krook (BGK) [**?**] for the classical Boltzmann equation provides a much simpler form of collision term and retains the principal effects of particle collisions and enables more tractable solution methods. The BGK

relaxation time concept is rather general and can be applicable to the semiclassical Boltzmann equation as well. The only change is that the equilibrium Maxwell-Boltzmann distribution in the classical case is replaced by the Bose-Einstein or Fermi-Dirac distribution depending on the types of carrier particles. The semiclassical Boltzmann-BGK equation has been widely applied for electron carrier transport in semiconductor [**?**,**?**,**?**,**?**,**?**,**?**,**?**,**?**,**?**] and phonon energy transport in thermoelectric materials [**?**]. Similarly, the solution methodology developed for classical Boltzmann-BGK equation can be applied to the semiclassical Boltzmann-BGK equation in phase space. In this work, we aim at developing an accurate direct solver for the semiclassical Boltzmann-BGK equation in phase space that can treat particles of three statistics on equal foot and in a parallel manner. Such a method will allow one to examine the same physical flow problems but with different gas of particles. It is noted that even when solving the problems for the classical Maxwell-Boltzmann statistics, the present formulation allows the analysis fugacity which has not been included in the original Boltzmann-BGK equation [**?**] nor in most of other existing works based on it. First, depending on the carrier particles, the discrete ordinate method is used to discretize the velocity (or momentum or wave number) space in the semiclassical Boltzmann-BGK equation into a set of equations for the discrete distribution functions which are continuous in physical space with source terms [**?**]. Second, the resulting equations can be treated as scalar hyperbolic conservation law with stiff source term whose evolution in space and time can be modeled by existing shock-capturing schemes such as total variation diminishing (TVD) schemes [**?**] and weighted essentially non-oscillatory (WENO) schemes [**?**]. The latter is adopted in this paper to describe the evolution of these equations. We develop the method in two space dimensions and validate the method using flow problems of one and two space dimensions. Three main aspects of the developed method are examined and emphasized, namely, the range of relaxation time, the range of Knudsen numbers and the recovery of the classical limit. After the success of these tests, the present method can provide a viable robust tool for treating many modern mesoscale carrier transport phenomena covering electrons and phonons in addition to the usual classical gas molecules. In the area of classical gas flows, the implementation of discrete ordinate method to nonlinear model Boltzmann equations has been developed by Yang and Huang [**?**] for the rarefied flow computations and has been able to cover broad range of flow regimes. Similar approaches using different high resolution spatial schemes were also given [**?**] [**?**]. In this work, the main purposes are first to explore the wide range of physical parameters of the semiclassical Boltzmann-BGK equation and second to examine the effects of particle statistics under the same flow problems. We adopt well established and previously developed spatial high resolution schemes such as TVD [**?**], NND [**?**], WENO [**?**]and compacted WENO [**?**] methods. Also to exclude the complexity due to solid boundary, we confine here to initial value problems. Under the same motivation as in classical case, the present work is built using discrete ordinate method to describe the hydrodynamic properties of rarefied gases of all the three statistics.

==========

In this work, we implement the high order discontinuous Galerkin method to solve the Boltzmann-BGK equation. The Discontinuous Galerkin method (DGM) is a special kind of finite element method. The main difference between the DGM and the continuous Galerkin method is that the DGM allows the nu-

merical to be discontinuous across the element edges and the resulting equations in the DGM are local to each element, [1, 2]. This difference enables us design high-order methods easily and renders the method highly parallelizable.

First, the discrete ordinate method is used to discretize the velocity (or momentum or wave number) space in the semiclassical Boltzmann-BGK equation into a set of equations for the discrete distribution functions which are continuous in physical space with source terms [**?**]. Second, the resulting equations in space into a set of semi-discrect equations using DG methods. The resulting ordinary differential equation system can be solved by Runge-Kutta methods.

However, the source term is stiff and it makes the explicit RK scheme inefficient. On the other hand, fully implicit schemes are expensive, especilly for multi-dimensonal or large-scale problems. Therefore, implicit-explicit (IMEX) Runge-Kutta methods are more appropriate for our problems and we consider the Additive Runge-Kutta (ARK) methods proposed by Kennedy and Carpenter [5] in this work.

==========

Elements of semiclassical Boltzmann-BGK equation is briefly described in Section 2. Its correlation with hydrodynamic equations is outlined. In Section 3, we describe the use of discrete ordinate method to discretize the particle distribution function into a set of hyperbolic conservation laws with source terms. In the next section, we present the description of fifth-order WENO scheme implementation in capturing the evolution of discretized distribution function equations. In Section 5, numerical experiments of one dimensional semiclassical gas dynamical flows in a shock tube in addition to two dimensional Riemann problems are presented to illustrate the present algorithm. Finally, concluding remarks will be given in Section 6.

2 Semiclassical Boltzmann-BGK Equation

In this section, we delineate the elements of semiclassical Boltzman-BGK equation which we expect to tackle in the present work. Following the works of [**?**, **?**], we consider the extension of the Boltzmann equation to quantum systems due to Uehling and Uhlenbeck in which they took the Pauli exclusion principle into account.

$$\left(\frac{\partial f}{\partial t}+\frac{\mathbf{p}}{m}\cdot\nabla_x-\nabla U(\mathbf{x},t)\cdot\nabla_{\mathbf{p}}\right)f(\mathbf{p},\mathbf{x},t)=\left(\frac{\delta f}{\delta t}\right)_{coll.} \tag{1}$$

where m is the particle mass, U is the mean field potential and $f(\vec{p},\vec{x},t)$ is the distribution function which represents the average density of particles with momentum $\vec{p}$ at the space-time point $\vec{x},t$. The $(\delta f/\delta t)_{coll.}$ denotes the collision term and according to Uehling and Uhlenbeck [**?**], it takes the form,

$$\begin{aligned}(\frac{\delta f}{\delta t})^{UU}_{coll.} &= \int d\mathbf{p}\int d\Omega K(\mathbf{p},\mathbf{q},\Omega)\{[1+\theta f(\mathbf{p},t)][1+\theta f(\mathbf{q})]f(\mathbf{p}^*,t)f(\mathbf{q}^*,t)\\ &\quad -[1+\theta f(\mathbf{p}^*,t)][1+\theta f(\mathbf{q}^*)]f(\mathbf{p},t)f(\mathbf{q},t)\},\end{aligned} \tag{2}$$

where $K(\mathbf{p},\mathbf{q},\Omega)$ denotes the collision kernel and Ω is the solid angle and θ is a parameter which specifies the type of particle statistics. Here, for $\theta=+1$, Bose-Einstein particles are considered, for $\theta=-1$, Fermi-Dirac particles, and

for $\theta = 0$, the Maxwell-Boltzmann classical particles are considered. According to the Boltzmann's H-theorem and conservation conditions, the collision integral of the semiclassical Boltzmann equation will automatically vanish when the distribution functions are in equilibrium and the equilibrium distribution function for general statistics can be expressed as

$$f^{eq}(\mathbf{p},\mathbf{x},t) = \frac{1}{z^{-1}\, exp\left\{\left[\mathbf{p} - m\,\mathbf{u}(\mathbf{x},t)\right]^2/2mk_BT(\mathbf{x},t)\right\} - \theta} \tag{3}$$

where $\mathbf{u}(\mathbf{x},t)$ is the mean velocity, $T(\mathbf{x},t)$ is temperature, k_B is the Boltzmann constant and $z(\mathbf{x},t) = exp\left(\mu(\mathbf{x},t)/k_BT(\mathbf{x},t)\right)$ is the fugacity, where μ is the chemical potential. In (3), $\theta = -1$ denotes the Fermi-Dirac statistics, $\theta = +1$, the Bose-Einstein statistics and $\theta = 0$ denotes the Maxwell-Boltzmann statistics. We note that even with the case of $\theta = 0$, we still have chemical potential μ or fugacity z which is rather different from the usual classical Maxwellian distribution. To avoid the mathematical difficulty caused by the nonlinear integral collision term , the relaxation time concept of Bhatnagar, Gross and Krook is generally applied to replace the collision term of Uehling and Uhlenbeck, thus the semiclassical Boltzmann-BGK equation reads

$$\left(\frac{\partial f}{\partial t} + \frac{\mathbf{p}}{m}\cdot\nabla_x - \nabla U(\mathbf{x},t)\cdot\nabla_{\mathbf{p}}\right) f(\mathbf{p},\mathbf{x},t) = \left(\frac{\delta f}{\delta t}\right)^{BGK}_{coll.} = -\,\frac{f - f^{eq}}{\tau} \tag{4}$$

Here, τ is the relaxation time and needs to be specified for each carrier scattering.

The macroscopic dynamic variables of interest such as number density, momentum density and energy density are low order moments of the distribution function and are defined by:

$$n(\mathbf{x},t) = \int \frac{d\mathbf{p}}{h^3}\, f(\mathbf{p},\mathbf{x},t)\,, \tag{5}$$

$$\mathbf{j}(\mathbf{x},t) = \int \frac{d\mathbf{p}}{h^3}\,\frac{\mathbf{p}}{m}\, f(\mathbf{p},\mathbf{x},t) = n(\mathbf{x},t)\,\mathbf{u}(\mathbf{x},t), \tag{6}$$

$$\epsilon(\mathbf{x},t) = \int \frac{d\mathbf{p}}{h^3}\,\frac{\mathbf{p}^2}{2m}\, f(\mathbf{p},\mathbf{x},t)\,. \tag{7}$$

where h is Planck's constant. Other higher-order moments such as stress tensor P_{ij} and the heat flux vector $\Phi_i(\mathbf{x},t)$ can also be defined accordingly as

$$P_{ij}(\mathbf{x},t) = \int \frac{d\mathbf{p}}{h^3}(\frac{p_i}{m} - u_i)(\frac{p_j}{m} - u_j)\, f(\mathbf{p},\mathbf{x},t), \tag{8}$$

$$\Phi_i(\mathbf{x},t) = \int \frac{d\mathbf{p}}{h^3}\,\frac{(\mathbf{p} - m\mathbf{u})^2}{2m}(\frac{p_i}{m} - u_i)\, f(\mathbf{p},\mathbf{x},t). \tag{9}$$

The conservation laws of macroscopic properties can be obtained by multiplying Eq. (1) respectively by 1, $\mathbf{p}$ and $\mathbf{p}^2/2m$ and integrating the resulting equations over all $\mathbf{p}$. Consequently, the integrals of the collision terms in all three cases vanish automatically resulting in the conservation laws in the form of differential equations for the conserved macroscopic quantities i.e., number

density $n(\mathbf{x},t)$, momentum density $mn\mathbf{u}(\mathbf{x},t)$, and energy density $\epsilon(\mathbf{x},t)$ as follow:

$$\frac{\partial n\left(\mathbf{x},t\right)}{\partial t} + \nabla_x \cdot \mathbf{j}\left(\mathbf{x},t\right) = 0, \tag{10}$$

$$\frac{\partial m\mathbf{j}\left(\mathbf{x},t\right)}{\partial t} + \nabla_x \cdot \int \frac{d\mathbf{p}}{h^3}\,\mathbf{p}\,\frac{\mathbf{p}}{m} f\left(\mathbf{p},\mathbf{x},t\right) = -n(\mathbf{x},t)\nabla_{\mathbf{x}} U(\mathbf{x},t), \tag{11}$$

$$\frac{\partial \epsilon\left(\mathbf{x},t\right)}{\partial t} + \nabla_x \cdot \int \frac{d\mathbf{p}}{h^3}\,\frac{\mathbf{p}}{m}\,\frac{\mathbf{p}^2}{2m} f\left(\mathbf{p},\mathbf{x},t\right) = -\mathbf{j}(\mathbf{x},t)\cdot\nabla_{\mathbf{x}} U(\mathbf{x},t). \tag{12}$$

Derivations of the semiclassical Euler and Navier-Stokes equations from the Boltzmann-BGK equation can be obtained from the zeroth order and first order solutions via the Chapman and Enskog expansion [**?**]. Also, the transport coefficients such as the viscosity η and the thermal conductivity κ can be derived in terms of the relaxation time as

$$\eta = \tau n k_B T \frac{\mathcal{Q}_2(z)}{\mathcal{Q}_1(z)}, \tag{13}$$

$$\kappa = \tau \frac{5k_B}{2m} n k_B T [\frac{7}{2}\frac{\mathcal{Q}_3(z)}{\mathcal{Q}_1(z)} - \frac{5}{2}\frac{\mathcal{Q}_2(z)}{\mathcal{Q}_1(z)}]. \tag{14}$$

where $\mathcal{Q}_\nu(z)$ is the Fermi or Bose function of order ν. For similar results derived from the linearized semiclassical Boltzmann equation, see [**?**]. Here the case of two space dimensions is assumed. The relaxation times for various scattering mechanisms of different carrier transport in semiconductor devices including electrons, holes, phonons and others have been proposed [15].

In this work, we will also consider the case of *semiclassical Euler* limit in which the particle distribution function is always in equilibrium, i.e., $f = f^{eq}$ and the collision term of Eq. (1) vanishes automatically. In the later section, we will present the comparison of our results with those of the semiclassical Euler solutions. In recent years, notable numerical methods to describe the ideal quantum gas flows have been developed, see [**?**, **?**, **?**].

2.1 Fermi and Bose functions in relation to hydrodynamics properties

Before we proceed, without losing generality, we neglect the influence of externally applied field $U(\mathbf{x},t)$. To illustrate the present method, we formulate the Fermi - Dirac equilibrium distribution in two spatial dimension as the following.

$$f^{eq}\left(p_x,p_y,x,y,t\right) = \frac{1}{z^{-1}\exp\left((p_x-mu_x)^2+(p_y-mu_y)^2\right)/(2mk_BT(x,y,t))+1} \tag{15}$$

In a closed form in terms of quantum functions, we replace the distribution function f with f^{eq} which automatically reduces the source term in the BGK Boltzmann equation to zero. The macroscopic moments, i.e., number density

$n(x,y,t)$, momentum $j(x,y,t)$ and energy density $\epsilon(x,y,t)$ are given by

$$\begin{aligned} n(x,y,t) &= \int\int \frac{dp_x\,dp_y}{h^2} f^{eq}(p_x,p_y,x,y,t) \\ &= \frac{\mathcal{Q}_1(z)^{\,2}}{\lambda} \end{aligned} \tag{16}$$

$$\begin{aligned} j_x(x,y,t) &= \int\int \frac{dp_x\,dp_y}{h^2} \frac{p_x}{m} f^{eq}(p_x,p_y,x,y,t) \\ &= n(x,y,t)u_x(x,y,t) \end{aligned} \tag{17}$$

$$\begin{aligned} j_y(x,y,t) &= \int\int \frac{dp_x\,dp_y}{h^2} \frac{p_y}{m} f^{eq}(p_x,p_y,x,y,t) \\ &= n(x,y,t)u_y(x,y,t) \end{aligned} \tag{18}$$

$$\begin{aligned} \epsilon(x,y,t) &= \int\int \frac{dp_x\,dp_y}{h^2} \frac{{p_x}^2+{p_y}^2}{2m} f^{eq}(p_x,p_y,x,y,t) \\ &= \frac{\mathcal{Q}_2(z)}{\beta\lambda^2} + \frac{1}{2}mn({u_x}^2+{u_y}^2) \\ &= \frac{P(x,y,t)}{(\gamma+1)} + \frac{1}{2}mn({u_x}^2+{u_y}^2) \end{aligned} \tag{19}$$

where $\lambda = \sqrt{\frac{\beta h^2}{2\pi m}}$ is the thermal wavelength and $\beta = 1/k_B T(x,y,t)$. The functions $\mathcal{Q}_\nu(z)$ of order ν are respectively defined for Fermi-Dirac and Bose-Einstein statistics as

$$\mathcal{F}_\nu(z) \equiv \frac{1}{\Gamma(\nu)}\int_0^\infty dx \frac{x^{\nu-1}}{z^{-1}e^x+1} \approx \sum_{l=1}^{\infty}(-1)^{l-1}\frac{z^l}{l^\nu} \tag{20}$$

$$\mathcal{B}_\nu(z) \equiv \frac{1}{\Gamma(\nu)}\int_0^\infty dx \frac{x^{\nu-1}}{z^{-1}e^x-1} \approx \sum_{l=1}^{\infty}\frac{z^l}{l^\nu} \tag{21}$$

Here, $\mathcal{F}_\nu(z)$ applies for Fermi-Dirac integral and $\mathcal{B}_\nu(z)$ for Bose-Einstein's, whereas $\Gamma(\nu)$ is gamma function. The definition of macroscopic quantities in terms of Fermi or Bose function applies for both cases of quantum distributions. One only needs to replace Fermi function with Bose function or vice versa whilst maintaining the same procedure.

2.2 Classical limit

Note that for $z \ll 1$, both $\mathcal{Q}_\nu(z)$ functions for all ν behave like z itself, i.e., $\mathcal{Q}_\nu(z) \approx z$. Physically, a large and negative value of chemical potential of a dilute system and high temperature environment do correspond to small z. On the other hand, we know that at the low temperature, the Fermi-Dirac case displays its most distinctive property in terms of one particle per one energy level mapping. We may intuitively say that the hydrodynamic properties of classical case can be acquired by replacing the $\mathcal{Q}_\nu(z)$ function into z itself. Mathematically, we can obtain the classical hydrodynamic properties by applying the same

procedure to the Maxwell-Boltzmann statistics as done to the other quantum statistics. For $\theta = 0$, the distribution function becomes

$$f^{MB}(p_x, p_y, x, y, t) = \\ 1/\left\{z^{-1} \exp\left\{\left[(p_x - mu_x)^2 + (p_y - mu_y)^2\right]/2mk_BT\right\}\right\}. \quad (22)$$

In this case, no approximation for $\mathcal{Q}_\nu(z)$ is required and the macroscopic values for two spatial dimensions can be obtained by

$$n_c(x, y, t) = \int\int \frac{dp_x\, dp_y}{h^2} f^{MB}(p_x, p_y, x, y, t) = \frac{z}{\lambda^2}. \quad (23)$$

In other words, in the classical limit,

$$z(x, y, t) = e^{\mu(x,y,t)/k_BT(x,y,t)} = \lambda^2\, n_c(x, y, t), \quad (24)$$

$$\mu(x, y, t) = k_BT(x, y, t) \ln(\lambda^2\, n_c(x, y, t)). \quad (25)$$

In the later section, we shall see the numerical examples that compare Fermi and Bose gas to the classical limit.

2.3 Normalization

Before proceeding to discretize the equation, in this section we introduce the characteristic properties of V_∞ and t_∞ for the purpose of normalization. The characteristic velocity and time can be defined as,

$$V_\infty = \sqrt{\frac{2k_BT_\infty}{m}}, \qquad t_\infty = \frac{L}{V_\infty}, \quad (26)$$

with L defined as the characteristic length of the problem. Hence the definitions of non-dimensional variables are introduced as

$$(\hat{t}, \hat{\tau}) = (t, \tau)/t_\infty,\ (\hat{u}_x, \hat{\upsilon_x}) = (u_x, \upsilon_x)/V_\infty,\ \hat{x} = x/L, \hat{T} = T/T_\infty$$
$$(\hat{u}_y, \hat{\upsilon_y}) = (u_y, \upsilon_y)/V_\infty,\ \hat{y} = y/L, \hat{n} = n/\left(\frac{m^2V_\infty^2}{h^2}\right)$$
$$\hat{j} = j/\left(\frac{m^2V_\infty^3}{h^2}\right),\ \hat{\epsilon} = \epsilon/\left(\frac{m^3V_\infty^4}{h^2}\right),\ \hat{f} = f. \quad (27)$$

Hence the normalized semiclassical Boltzmann-BGK equation,

$$\frac{\partial \hat{f}(\hat{\upsilon}_x, \hat{\upsilon}_y, \hat{x}, \hat{y}, \hat{t})}{\partial \hat{t}} + \hat{\upsilon}_x \frac{\partial \hat{f}(\hat{\upsilon}_x, \hat{\upsilon}_y, \hat{x}, \hat{y}, \hat{t})}{\partial \hat{x}} + \hat{\upsilon}_y \frac{\partial \hat{f}(\hat{\upsilon}_x, \hat{\upsilon}_y, \hat{x}, \hat{y}, \hat{t})}{\partial \hat{y}} = -\frac{\hat{f} - \hat{f}^{eq}}{\hat{\tau}} \quad (28)$$

with $\hat{\upsilon}_x$ and $\hat{\upsilon}_y$ as particle velocities. Neglecting the *hat* sign, the normalized two-dimensional semiclassical equilibrium distribution function becomes

$$f^{eq}(\upsilon_x, \upsilon_y, x, y, t) = \frac{1}{z^{-1} \exp\left((\upsilon_x - u_x)^2 + (\upsilon_y - u_y)^2\right)/T + \theta} \quad (29)$$

3 Application of Discrete Ordinate Method

As applied by Huang and Giddens [**?**] and Shizgal [**?**] to the linearized Boltzmann-BGK equation, the discrete ordinate method represents functions by a set of

discrete points that coincide with the evaluation points in a quadrature rule. The method replaces the original functional dependency on the integral variable by a set of functions with N elements of $W_i f(x_i)$ with $i = 1, \ldots, N$. The points x_i are quadrature points and W_i are the corresponding weights of the integration rule

$$\int_a^b W(x) f(x) dx = \sum_{i=1}^{N} W_i f(x_i). \tag{30}$$

The interval $[a, b]$ will be either $[0, \infty]$ or $[-\infty, \infty]$ depending on considered application. Different weighting function $W(x)$ is addressed accordingly. In general, in view of the fact that in the classical limit all three statistics will coincide with each other, we shall employ the Gauss-Hermite quadrature for all three statistics. This method is beneficial given the fact that in the end, we are not just interested in the distribution function itself but also in the macroscopic moments and the evaluations of the macroscopic moments are also done with the same quadrature. The discrete ordinate method has been applied to the classical nonlinear model Boltzmann equations for rarefied flow computations [**?**]. By applying the discrete ordinate method to the equation (28), the distribution function in phase space $f(\upsilon_x, \upsilon_y, x, y, t)$ can be rendered into a set of hyperbolic conservation equation with source terms for $f_{\sigma,\delta}(x, y, t)$ in the physical space, where $\sigma = -N_1, \ldots, -1, 1, \ldots, N_1$ and $\delta = -N_2, \ldots, -1, 1, \ldots, N_2$. The resulting equations are a set of

$$\frac{\partial f_{\sigma,\delta}(x, y, t)}{\partial t} + \nabla \cdot (\upsilon_{\sigma,\delta}\, f_{\sigma,\delta}(x, y, t)) = -\frac{f_{\sigma,\delta} - f^{eq}}{\tau} \tag{31}$$

with $f_{\sigma,\delta}$ and $\upsilon_{\sigma,\delta} =< \upsilon_\sigma, \upsilon_\delta >$ represent the values of f and $< \upsilon_x, \upsilon_y >$ evaluated at the discrete velocity points σ and δ, respectively.

3.1 Quadrature Methods

In two-dimensional case, we may apply Gauss-Hermite quadrature rule over the interval $[-\infty, \infty]$. The Gauss-Hermite quadrature rule reads,

$$\int_{-\infty}^{\infty}\int_{-\infty}^{\infty} e^{-\upsilon_x{}^2} e^{-\upsilon_y{}^2} f(\upsilon_x, \upsilon_y) d\upsilon_x\, d\upsilon_y \approx \sum_{\sigma=-N_1}^{N_1} \sum_{\delta=-N_2}^{N_2} W_\sigma\, W_\delta\, f_{\sigma,\delta} \tag{32}$$

or

$$\int_{-\infty}^{\infty}\int_{-\infty}^{\infty} e^{-\upsilon_x{}^2} e^{-\upsilon_y{}^2} [e^{\upsilon_x{}^2} e^{\upsilon_y{}^2} f(\upsilon_x, \upsilon_y) d\upsilon_x\, d\upsilon_y] \approx$$

$$\sum_{\sigma=-N_1}^{N_1} \sum_{\delta=-N_2}^{N_2} W_\sigma\, W_\delta\, e^{\upsilon_\sigma{}^2} e^{\upsilon_\delta{}^2} f_{\sigma,\delta} \tag{33}$$

The discrete points υ_α and weight W_α, with $\alpha = \sigma, \delta$, are tabulated in the table of the Gauss-Hermite quadrature, see [**?**] and can be found through

$$W_\alpha = \frac{2^{l-1} l! \sqrt{\pi}}{l^2 [H_{l-1}(\upsilon_\alpha)]^2} \tag{34}$$

with l is number of quadrature points and υ_α are the roots of the Hermite polynomial $H_l(\upsilon)$ Once the discretized functions $f_{\sigma,\delta}(x, y, t)$ are solved, for every

time level we can acquire and update the macroscopic moments in the physical space using a selected quadrature method as described below.

$$\begin{aligned} n(x,y,t) &= \int_{-\infty}^{\infty} [f(\upsilon_x,\upsilon_y,x,y,t) e^{{\upsilon_x}^2} e^{{\upsilon_y}^2}] e^{-{\upsilon_x}^2} e^{-{\upsilon_y}^2} d\upsilon_x d\upsilon_y \\ &= \sum_{\sigma=-N_1}^{N_1} \sum_{\delta=-N_2}^{N_2} W_\sigma \, W_\delta \, e^{{\upsilon_\sigma}^2} e^{{\upsilon_\delta}^2} f_{\sigma,\delta} \end{aligned} \tag{35}$$

$$\begin{aligned} j_x(x,y,t) &= \int_{-\infty}^{\infty} [\upsilon_x \, f(\upsilon_x,\upsilon_y,x,y,t) e^{{\upsilon_x}^2} e^{{\upsilon_y}^2}] e^{-{\upsilon_x}^2} e^{-{\upsilon_y}^2} d\upsilon_x d\upsilon_y \\ &= \sum_{\sigma=-N_1}^{N_1} \sum_{\delta=-N_2}^{N_2} \upsilon_\sigma \, W_\sigma \, W_\delta \, e^{{\upsilon_\sigma}^2} e^{{\upsilon_\delta}^2} f_{\sigma,\delta} \\ &= n(x,y,t) \, u_x(x,y,t) \end{aligned} \tag{36}$$

$$\begin{aligned} \epsilon(x,y,t) &= \int_{-\infty}^{\infty} [\frac{\upsilon_x^2+\upsilon_y^2}{2} f(\upsilon_x,\upsilon_y,x,y,t) e^{{\upsilon_x}^2} e^{{\upsilon_y}^2}] e^{-{\upsilon_x}^2} e^{-{\upsilon_y}^2} d\upsilon_x d\upsilon_y \\ &= \sum_{\sigma=-N_1}^{N_1} \sum_{\delta=-N_2}^{N_2} (\frac{\upsilon_\sigma^2+\upsilon_\delta^2}{2}) W_\sigma \, W_\delta \, e^{{\upsilon_\sigma}^2} e^{{\upsilon_\delta}^2} f_{\sigma,\delta} \end{aligned} \tag{37}$$

Pressure $P(x,y,t)$ can be defined as

$$P(x,y,t) = [\epsilon(x,y,t) - \frac{1}{2} n(x,y,t)(u_x^2+u_y^2)](\gamma-1) \tag{38}$$

The value of relaxation time is given by

$$\tau = \eta / P \tag{39}$$

Here, we note that the basic criteria of choosing different quadratures is to guarantee that the macroscopic moments can be accurately computed which requiring the accurate representation of the distribution function with suitable velocity range being covered. The equally spaced Newton-Cotes formula can also be used if one needs to cover the high energy tail of the distribution function.

4 Numerical Method

4.1 Application of Discontionuous Galerkin Methods

In this section, we describe the numerical algorithm to solve the set of equations (31). A class of DGM is implemented to solve the set of conservation laws with source terms.

On each element K in a partition, $T_h = \{K_n\}$, of the computational domain $\Omega \subset \mathbb{R}^2$, we consider local spaces $U(K) = Q^k(K)$ consisting of polynomials of degree smaller than or equal to k. To construct the DG scheme, we first consider the weak form of the equation on each element K: for all $g \in U(K)$

$$\int_K \frac{\partial f_{\sigma,\delta}}{\partial t} \, g \, dA + \int_K \nabla \cdot (\upsilon_{\sigma,\delta} \, f_{\sigma,\delta}) \, g \, dA = - \int_K (\frac{f_{\sigma,\delta} - f^{eq}}{\tau}) \, g \, dA$$

or

$$\int_K \frac{\partial f_{\sigma,\delta}}{\partial t}\, g\, dA - \int_K (v_{\sigma,\delta}\, f_{\sigma,\delta})\cdot\nabla\, g\, dA + \int_{\partial K} (v_{\sigma,\delta}\, f_{\sigma,\delta})\cdot\mathbf{n}\, g\, ds = -\int_K (\frac{f_{\sigma,\delta} - f^{eq}}{\tau})\, g\, dA.$$

Replace $v_{\sigma,\delta}\, f_{\sigma,\delta}$ by the numerical flux $\widehat{v_{\sigma,\delta}\, f_{\sigma,\delta}}$ and we have the the DG scheme. On each element K, for all $g \in U(K)$, we look for a numerical solution $f_{\sigma,\delta}$ satisfying

$$\int_K \frac{\partial f_{\sigma,\delta}}{\partial t}\, g\, dA - \int_K (v_{\sigma,\delta}\, f_{\sigma,\delta})\cdot\nabla\, g\, dA + \int_{\partial K} \widehat{v_{\sigma,\delta}\, f_{\sigma,\delta}}\cdot\mathbf{n}\, g\, ds = -\int_K (\frac{f_{\sigma,\delta} - f^{eq}}{\tau})\, g\, dA. \tag{40}$$

for all σ and δ.

The choice of the numerical flux is crucial in the design of the DG scheme and is related to the stability of the numerical scheme. In this work, we consider the up-winding numerical flux,

$$\widehat{v_{\sigma,\delta}\, f_{\sigma,\delta}} = v_{\sigma,\delta}\, \{\!\{f_{\sigma,\delta}\}\!\} + \frac{1}{2}|v_{\sigma,\delta}\cdot\mathbf{n}|[\![f_{\sigma,\delta}]\!]$$

where Please see [2] for other numerical fluxes.

Then we write the numerical solution in the basis form, $f_{\sigma,\delta}|_K(t,x,y) = a_i(t)\phi_i(x,y)$, and, on each K, we have, for $j = 0, ..., k$,

$$\begin{aligned} &\int_K (a_i)_t \phi_i(x,y)\phi_j(x,y)\, dA - \int_K v_{\sigma,\delta}\, a_i \phi_i(x,y)\cdot\nabla\phi_j(x,y)\, dA \\ + \quad &\int_{\partial K} \widehat{v_{\sigma,\delta}\, f_{\sigma,\delta}}\cdot\mathbf{n}\phi_j(x,y)\, ds = -\int_K (\frac{f_{\sigma,\delta} - f^{eq}}{\tau})\, \phi_j(x,y)\, dA. \end{aligned} \tag{41}$$

The above semi-discrete equations can be written in the form of a set of ordinary differential equations,

$$M\frac{d}{dt}U = NU + S(U).$$

We can then solve the above ODE system using Runge-Kutta methods. Note that the matrix M is identity or block-diagonal and we can solve the system without inverting a big matrix.

4.2 Additive Runge-Kutta Methods

In this paper, we consider a fourth order six-stage ARK_2 method, proposed by C.A.Kennedy and M.H.Carpenter [**?**]. Eq. (41) can be cast in the form

$$\frac{dU}{dt} = F_{ns} + F_s$$

where F_{ns} represents the nonstiff term, which corresponds to the convection term, and F_s represents the stiff term, which corresponds to the source term.

In this methods, we integrate the nonstiff terms with a explicit Runge-Kutta method (ERK) and treat the stiff term with singly diagonally implicit Runge-Kutta method with an explicit first stage(ESDIRK).

Coefficients for the ERK and ESDIRK methods are represented by the Butcher tableau and given in the appendix,

$$\begin{array}{c|ccccccc}
0 & 0 & 0 & 0 & 0 & \dots & 0 \\
2\gamma & 2\gamma & 0 & 0 & 0 & \dots & 0 \\
c_3 & a_{31}^{[E]} & a_{32}^{[E]} & 0 & 0 & \ddots & \vdots \\
\vdots & \vdots & \vdots & \ddots & \ddots & \ddots & 0 \\
c_{s-1} & a_{s-1,1}^{[E]} & a_{s-1,2}^{[E]} & a_{s-1,3}^{[E]} & \dots & 0 & 0 \\
1 & a_{s,1}^{[E]} & a_{s,1}^{[E]} & a_{s,1}^{[E]} & \dots & a_{s,s-21}^{[E]} & 0 \\
\hline
 & b_1 & b_2 & b_3 & \dots & b_{s-1} & \gamma
\end{array}
\qquad
\begin{array}{c|ccccccc}
0 & 0 & 0 & 0 & 0 & \dots & 0 \\
2\gamma & \gamma & \gamma & 0 & 0 & \dots & 0 \\
c_3 & a_{31}^{[I]} & a_{32}^{[I]} & \gamma & 0 & \ddots & \vdots \\
\vdots & \vdots & \vdots & \ddots & \ddots & \ddots & 0 \\
c_{s-1} & a_{s-1,1}^{[I]} & a_{s-1,2}^{[I]} & a_{s-1,3}^{[I]} & \dots & \gamma & 0 \\
1 & b_1 & b_2 & b_3 & \dots & b_{s-1} & \gamma \\
\hline
 & b_1 & b_2 & b_3 & \dots & b_{s-1} & \gamma
\end{array}$$

where the superscript $[E]$ and $[I]$ denote the coefficients for the explicit and implicit methods, respectively,

Let $F_{ns}^{(j)}$ and $F_s^{(j)}$ approximate $F_{ns}(U^{(j)}, t^n + c_j\Delta t)$ and $F_s(U^{(j)}, t^n + c_j\Delta t)$, respectively. The numerical solution at t^{n+1} is given by

$$U^{n+1} = U^n + \Delta t \sum_{i=1}^{s} b_i \big(F_s^{(i)} + F_{ns}^{(i)}\big). \tag{42}$$

To get the inter-stage solution $U^{(i)}$, we solve

$$U^{(i)} = U^{(n)} + X^{(i)} + \Delta t\gamma F_s^{(i)}, \quad i \geq 2, \tag{43}$$

where $X^{(i)} = \Delta t \sum_{j=1}^{i-1} \left(a_{ij}^{[E]} F_{ns}^{(j)} + a_{ij}^{[I]} F_s^{(j)}\right)$ is explicitly computed from the existing data.

4.3 Calculate the values of z and T

After acquiring the macroscopic moments, we need to update the values of z and T. To solve $z(x, y, t)$, which is the root of equation

$$\Psi_2(z) = 2\epsilon - \frac{\mathcal{Q}_2(z)}{\pi}\left(\frac{n}{\mathcal{Q}_1(z)}\right)^2 - n(u_x^2 + u_y^2) \tag{44}$$

we can use a range of numerical root finding methods. Note that Eq. (44) can be derived from Eqs. (16)-(19). In this paper, the bisection method is used to solve z from Eq. (44). After z is acquired, we can immediately find T before advancing to the solution of the next time step.

5 Computational Results

In this section we present the results of selected two-dimensional Riemann problems. The domain is discretized into a collection of rectangles and a typical mesh is shown in Figure 1. We choose Legendre polynomials as basis to generate the local function space and implement a quadrature-free RKDG method, [3], to accelerate the computation. However, numerical integrations are still needed for the computations of the source terms.

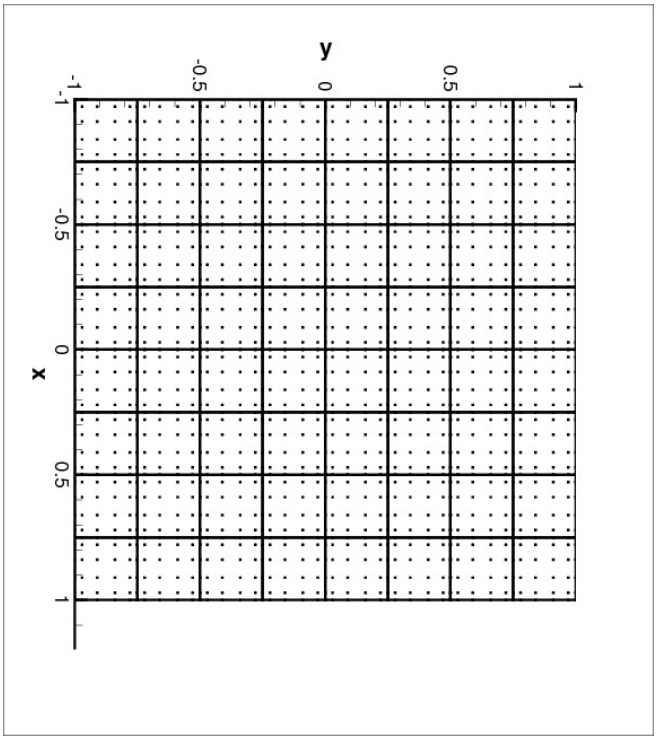

Figure 1: A mesh consists of 64 elements

5.1 Two-dimensional Riemann problems

Following the works of Lax and Liu, [**?**] and Schultz-Rinne et al. [**?**], we selected several configurations to be tested among those of the above-cited papers. In the Riemann problems of two-dimensional gas dynamics, the initial state is in equilibrium and kept constant in each of the four quadrants. See the illustration in Fig. **??**. The set up is made so that only one elementary wave, a 1-D shock, $\vec{S}$, a 1-D rarefaction wave, $\vec{R}$, or a 2-D contact discontinuity, J, appears at each interface. To satisfy these constraints, the set initial data must satisfy the Rankine-Hugoniot relations i.e., for a given left an right state (denoted by the indices l and r), we define

$$\Phi_{lr} = \frac{2\sqrt{\gamma}}{\gamma-1}\left(\sqrt{\frac{P_l}{n_l}}-\sqrt{\frac{P_r}{n_r}}\right) \tag{45}$$

$$\Psi_{lr}^2 = \frac{(P_l-P_r)(n_l-n_r)}{n_l n_r}, \qquad (\Psi_{lr}>0) \tag{46}$$

$$\Pi_{lr} = \left(\frac{P_l}{P_r}+\frac{(\gamma-1)}{(\gamma+1)}\right)/\left(1+\frac{(\gamma-1)P_l}{(\gamma+1)P_r}\right) \tag{47}$$

For cases that include rarefaction waves or shocks, these equations are respectively applied,

$$n_l/n_r = (P_l/P_r)^{1/\gamma} \quad \text{or} \quad n_l/n_r = \Pi_{lr} \tag{48}$$

In this two-dimensional formulation, $\gamma = 2$ is chosen. The quadrature rule used is Gauss-Hermite rule with 20 abscissas both in υ_x and υ_y directions.

5.2 Configuration 13

In this subsection, we test the class of 2-D Riemann's problem with the following initial set up for configuration 13,

$$J_{21}, \overleftarrow{S_{32}}, J_{34}, \overrightarrow{S_{41}}, \quad P_1 = P_2 > P_3 = P_4 \tag{49}$$

$$u_{x1} = u_{x2} = u_{x3} = u_{x4} \tag{50}$$

$$u_{y4} - u_{y1} = \Psi_{41}, \qquad u_{y3} - u_{y2} = \Psi_{32} \tag{51}$$

The initial conditions set in the four quadrants are

$$\begin{array}{llll} z_2 = 0.4253 & u_{y2} = 0.3 & z_1 = 0.142 & u_{y1} = -0.3 \\ u_{x2} = 0 & T_2 = 1.1494 & u_{x1} = 0. & T_1 = 2.0782 \\ z_3 = 0.4448 & u_{y3} = 0.697 & z_4 = 0.151 & u_{y4} = 0.26254 \\ u_{x3} = 0 & T_3 = 0.7083 & u_{x4} = 0 & T_4 = 1.273 \end{array} \tag{52}$$

5.3 Configuration 17

$$J_{21}, \overleftarrow{S_{32}}, J_{34}, \overrightarrow{R_{41}}, \quad P_1 = P_2 > P_3 = P_4 \tag{53}$$

$$u_{x1} = u_{x2} = u_{x3} = u_{x4} \tag{54}$$

$$u_{y4} - u_{y1} = \Phi_{41}, \qquad u_{y3} - u_{y2} = \Psi_{32} \tag{55}$$

$$\begin{array}{llll} z_2 = 0.37 & u_{y2} = -0.3 & z_1 = 0.14 & u_{y1} = -0.4 \\ u_{x2} = 0 & T_2 = 1.25 & u_{x1} = 0.1 & T_1 = 2.08 \\ z_3 = 0.38 & u_{y3} = 0.12 & z_4 = 0.14 & u_{y4} = -0.98 \\ u_{x3} = 0 & T_3 = 0.77 & u_{x4} = 0 & T_4 = 1.31 \end{array} \tag{56}$$

5.4 Configuration 5

$$J_{21}, J_{32}, J_{34}, J_{41}, \quad P_1 = P_2 = P_3 = P_4 \tag{57}$$

$$u_{x1} = u_{x2} < u_{x3} = u_{x4}, \qquad u_{y1} = u_{y4} < u_{y3} = u_{y2} \tag{58}$$

$$\begin{array}{llll} z_2 = 0.4253 & u_{y2} = 0.5 & z_1 = 0.142 & u_{y1} = -0.5 \\ u_{x2} = -0.75 & T_2 = 1.1494 & u_{x1} = -0.75 & T_1 = 2.078 \\ z_3 = 0.142 & u_{y3} = 0.5 & z_4 = 0.6635 & u_{y4} = -0.5 \\ u_{x3} = 0.75 & T_3 = 2.078 & u_{x4} = 0.75 & T_4 = 0.8768 \end{array} \tag{59}$$

6 Concluding Remarks

- Observation
  1. For corse meshes, Figure **??**, there are some jumps across the element edges and the jumps diminished when the number of elements increased to 256 elements. (Need 3D plots)
  2. No slope limiter or artificial filter are implemented. Since the intial setup is not smooth, there are oscillations in the beginning. However, the oscillations are diminished as time evoloves due to the kinetic property of the problem. (Need 3D plots near the beginning)
  3. (Convergence) Take the result of the TVD scheme with 800×800 grid points as the reference solution, we can see the solutions, Figure **??** - Figure **??**, of the DG methods converge to the reference solution.
  4. From Figure **??**, Figure **??** and Figure **??**, we can see that the performances of DG and WENO schemes are better than the TVD scheme and DG scheme is slightly better than the WENO. Note the unknowns of the three methods are the same (64×64)
- Issues
  1. Time-Step Size (Stability): For the scheme to be stable, there is a limit for the time-step size,
  $$\Delta t < \frac{1}{C_a + C_s},$$
  where C_a is related to the stability of the linear advection and can be found at [1]. C_s is related to the source term and, theoretically, we can estimate it by linearization. However, a good estimate of C_s is not easy to get and a rough estimate gives us a very small time step. Anyway, the source term is stiff in time integration and it's better to solve it implicitly. Therefore we should consider implicit-explicit Runge-Kutta methods.
  2. (Oscillations) Although the oscillations are diminished as time evoloves due to the kinetic property, the oscillations may affect the stability.

References

[1] B. Cockburn and C.-W. Shu, *Runge-Kutta discontinuous Galerkin methods for convection-dominated problems*, J. Sci. Comput. **16** (2001), 173–261.

[2] B. Cockburn (2003) *Discontinuous Galerkin methods,* Journal of Applied Mathematics and Mechanics, 83, pp 731-754.

[3] Min-Hung Chen, Po-Yu Shieh *A High-Order Quadrature-Free RKDG Method for Wave Equations on Structured Grids With GPU Acceleration*, in preparation.

[4] M. CARPENTER and C. KENNEDY, *Fourth-Order 2N-Storage Runge-Kutta Schemes*, NASA TM 109112, NASA Langley Research Center, June 1994.

[5] C.A.Kennedy, M.H.Carpenter, Additive Runge-Kutta schemes for convection-diffusion-reaction equations, Appl.Numer.Math. 44(2003) 139-181.

1. **ARK4(3)6L[2]SA-ERK**

0	0	0	0	0	0	0
$\frac{1}{2}$	$\frac{1}{2}$	0	0	0	0	0
$\frac{83}{250}$	$\frac{13861}{62500}$	$\frac{6889}{62500}$	0	0	0	0
$\frac{31}{50}$	$\frac{-1169233316275}{2393684061468}$	$\frac{-2731218467317}{153680421018831}$	$\frac{9408046702089}{111131711139209}$	0	0	0
$\frac{17}{20}$	$\frac{-451086348788}{2902428689909}$	$\frac{-2682348792572}{7519795681897}$	$\frac{12662868775082}{11960479115383}$	$\frac{3355817975965}{11060851509271}$	0	0
1	$\frac{647845179188}{3216320057751}$	$\frac{73281519250}{8382639484533}$	$\frac{552539513391}{34546683862333}$	$\frac{3354512671639}{8306763924573}$	$\frac{4040}{17871}$	0
	$\frac{82889}{524892}$	0	$\frac{15625}{83664}$	$\frac{69875}{102672}$	$\frac{-2260}{8211}$	$\frac{1}{4}$

2. **ARK4(3)6L[2]SA-ESDIRK**

0	0	0	0	0	0	0
$\frac{1}{2}$	$\frac{1}{4}$	$\frac{1}{4}$	0	0	0	0
$\frac{83}{250}$	$\frac{8611}{6250}$	$\frac{-1743}{31250}$	$\frac{1}{4}$	0	0	0
$\frac{31}{50}$	$\frac{5012029}{34652500}$	$\frac{-654441}{2922500}$	$\frac{174375}{388108}$	$\frac{1}{4}$	0	0
$\frac{17}{20}$	$\frac{15267082809}{155376265600}$	$\frac{-71443401}{120774400}$	$\frac{730878875}{902184768}$	$\frac{2285395}{8070912}$	$\frac{1}{4}$	0
1	$\frac{82889}{524892}$	0	$\frac{15625}{83664}$	$\frac{69875}{102672}$	$\frac{-2260}{8211}$	$\frac{1}{4}$
	$\frac{82889}{524892}$	0	$\frac{15625}{83664}$	$\frac{69875}{102672}$	$\frac{-2260}{8211}$	$\frac{1}{4}$